Large-scale Modeling and DR Control of Electric Water Heaters with Energy Star and CTA-2045 Control Types in Distribution Power Systems

Huangjie Gong, *Student Member, IEEE*, Evan S. Jones, *Student Member, IEEE*, A H M Jakaria, Aminul Huque, *Member, IEEE*, Ajit Renjit, *Member, IEEE* and Dan M. Ionel, *Fellow, IEEE*

Abstract: The paper proposes a generalized energy storage (GES) model for battery energy storage systems (BESS), electric water heaters (EWH) and heating, ventilation, and air-conditioning (HVAC) systems to enable demand response control complying to Energy Star and CTA-2045 standards. The demand response control has been implemented in the DER integration testbed, which was originally developed by EPRI, to demonstrate that the "energy content" and "energy take" for BESS and EWH with mixing valve technology are comparable for typical residential ratings. A distribution power system was modeled using the modified IEEE 123-bus feeder system, measured residential loads, and EWH power simulated based on realistic hot water draws from CBECC-Res software. The demand response control, which complies to CTA-2045 standards was implemented to the EWHs considering the energy take values. Results demonstrate that the EWHs can be controlled to postpone the peak power at the distribution system level and provide a large amount of energy storage, while maintaining system robustness. The impact on occupant comfort was also analyzed.

***Index Terms*—Battery Energy Storage System (BESS), Electric Water Heater (EWH), Alternative Energy Storage, ANSI/CTA-2045-B, Energy Star, Energy Take, Home Energy Management (HEM), Demand Response (DR), Power System, OpenDSS, IEEE 123-bus, Voltage Variation.**

I. Introduction

The advancement of smart home and grid technologies and the associated electric power system integration studies relies on individual and combined simulators for buildings, such as EnergyPlus, and circuit networks, e.g., OpenDSS, MATPOWER, GridLAB-D, etc. [1]. The Distributed Energy Resources (DER) integration testbed, which includes open-source simulation software, was originally developed by the Electric Power Research Institute (EPRI), comprises multiple layers for controls, devices, and circuits, and is able to communicate using protocols that are typically employed for hardware components [2], [3]. Using this technique, the DER integration testbed can be used with a combination of real physical devices and/or with their equivalent model-in-the-loop (MIL) software implementation. The advantages of the MIL approach include cost-effective development and testing in a realistic set-up and the ability to largely scale-up studies with minimal hardware [4], [5].

The Message Queuing Telemetry Transport (MQTT) is a widely used messaging protocol for the communication of internet-of-things (IoT) [6]. In this study, MQTT connects separate devices to the network simulator from both measurement and simulation software, which enables the MIL. The MQTT message middleware makes possible the reliable data transmission among sensing and the application service layers, realizing the home energy management system [7] devices.

Energy storage devices and systems, which can be electric, such as battery energy storage systems (BESS), or thermal, such as electric water heaters (EWH) or heating, ventilation and air conditioning (HVAC) systems [8], are essential in order to ensure an optimal energy management and power flow within the modern grid with DER. This method of hybrid energy storage can reduce required BESS capacity by up to 30% while providing the same capability [9]. To support technology development and standard-type implementation that would enable wide scale industrial and utility deployment, Energy Star, a program conducted by the Environmental Protection Agency (EPA) and Department of Energy (DOE), provides general specifications for energy parameters and demand response (DR) functionalities [10].

For EWH, these specifications are typically implemented using the Consumer Technology Association (CTA) 2045 standard [11], and success has been reported at the individual residential and utility aggregated levels [12], [13]. In principle, the combined Energy Star and CTA-2045 specifications and concepts such as "energy capacity", "energy content", and "energy take" and DER commands, such as "load up", "shed", etc., can be extended to any energy storage device and system, enabling a unified approach at the system level.

Modeling of EWH energy use at the individual level to be employed in a DER testbed may be performed through physics-based equations to model the thermal losses to the environment and water consumption as well as for the contribution from the heating element [14]. In addition to these

H. Gong, E. S. Jones, and D. M. Ionel are with the SPARK Laboratory, Department of Electrical and Computer Engineering, University of Kentucky, Lexington, KY, USA (e-mail: huangjie.gong@uky.edu, sevanjones@uky.edu, dan.ionel@ieee.org).

A H M Jakaria, Aminul Huque, and Ajit Renjit are with Tennessee Valley Authority, USA (e-mails: ajakaria@epri.com, mhuque@epri.com, arenjit@epri.com).

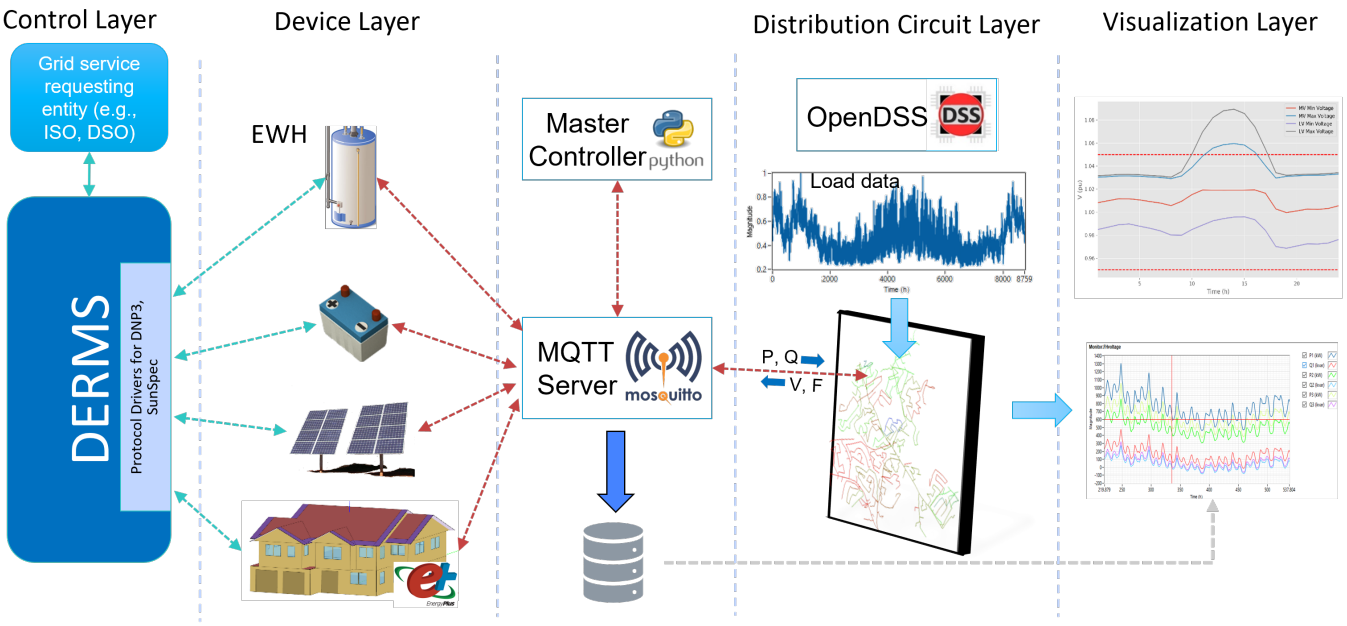

Figure 1. The architecture of EPRI's DER integration testbed. Models-in-the-loop (MIL) are employed at the device layer. The paper proposes unified models for the battery energy storage systems (BESS) and electric water heaters (EWH) suitable for Energy Star and CTA-2045 control types, which are issued by a distributed energy resource management system (DERMS). The MILs are to communicate with the distribution system simulator, which is OpenDSS for this study, through the Message Queuing Telemetry Transport (MQTT), which enables distribution-level simulation of control schemes.

mathematical representations, estimation through measured data was utilized to determine certain parameters of the physical model. Typical domestic hot water (DHW) schedules, such as those provided by the CBECC-Res Compliance Software Project [15], are very useful resources for performing realistic community-level simulation studies.

The IEEE test bus systems are available in OpenDSS for the studies of large scale DER implementation and DR control [16], [17]. These distribution system models in combination with proper control strategies and by considering the behavior of EWHs in an aggregated manner enables the community-level study of EWHs as controllable residential BESSs. When deployed as an aggregate entity, EWHs can be considered assets for grid services [18]. It has been shown that EWHs at aggregated level can provide equivalent grid service as batteries [19].

A research gap remains for large scale simulation of EWHs in a distribution power system. A study to help with this gap in literature should fulfill three important criteria. First, each EWH should have its own hot water draw, which should be realistic and representative of typical usage. Second, the impact of DR control on EWHs should also consider both power demand and the voltages of buses at which the associated residences are connected. Also, the change of total load in the power system should consider the power losses. Third, the DR control signals for EWHs should comply with the CTA-2045 standards.

This paper is a substantially expanded follow up of a previous conference paper by the same research group, which introduced the EPRI's DER testbed and defined the GES concept including EWH and BESS [20]. In addition to the previous conference paper, EWHs were simulated on a large scale each with their own daily hot water draw in the expansion. The modified IEEE 123-bus feeder system was simulated with residences comprising of measured load data and simulated EWH power. The DR control complying to CTA-2045 standard was tested and discussed.

The main contributions include: (1) verification of EWHs as equivalent energy storage and the evaluation of the energy storage capacity; (2) a proposed method for batch modeling of individual EWHs based on realistic hot water flow; (3) combined dynamic simulation of individual EWHs and a distribution power system with realistic residential loads; (4) application of CTA-2045 standard-based DR on EWH at a large scale; (5) the analysis of EWH DR impact on an example distribution power system, including peak reduction and voltage variation.

Following the introduction, the EPRI DER testbed is introduced, and the GES concept is then defined in Section II. Case studies that apply the EWH as energy storage are presented in Section III. The modeling for multiple EWHs with realistic DHW draw is provided in Section IV. Results for the co-simulation of EWHs and the distribution power system are presented and discussed in Sections V and VI. The final section includes the conclusions of this work.

II. EPRI's DER Integration Testbed and Definitions of Generalized Energy Storage

The EPRI's DER integration testbed (Fig. 1) simulates power system models with real world communication systems

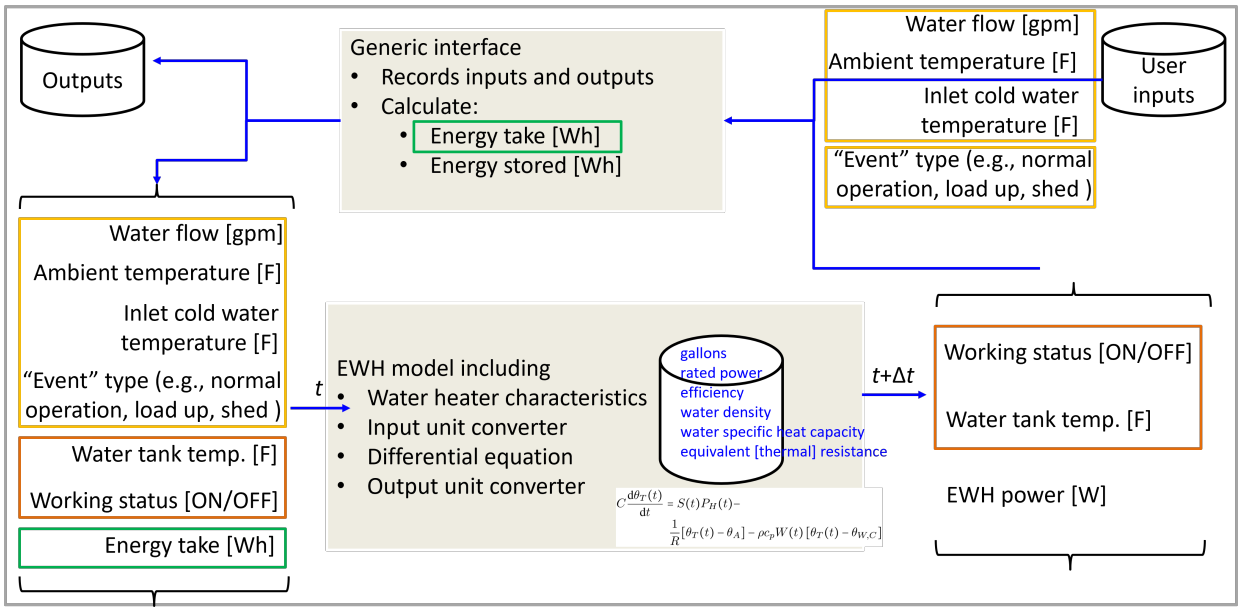

Figure 2. Schematic of the Model-In-the-Loop (MIL) for an Electric Water Heater (EWH). The computer code is implemented in C# under Visual Studio 2020 and communications with the EPRI's DER integration testbed follow the CTA-2045 standard for Energy Star commands. This model is plugged into the EPRI's DER integration testbed (Fig. 1) as EWH in the "Device Layer".

and DER models. The testbed can assess the control functionality and communication interoperability of the Distributed Energy Resources Management System (DERMS) and can evaluate different control strategies for any circuit. It also supports real world communication systems by incorporating industry standard protocols, such as the CTA-2045 standard, Energy Star specifications, DNP3, and SunSpec Modbus.

EPRI's DER testbed has four layers in its overall architecture, including control, device, circuit, and visualization and analytics (Fig. 1). The control layer contains the EPRI-developed reference control tool OpenDERMS, which can aggregate, optimize, and manage a large number of DERs to provide grid services and enable customer benefits. It is within this layer that the CTA-2045 protocol is utilized such that controls issued by OpenDERMS are applicable to all such DERs in the device layer. Consolidating control methods in this way enables the consideration of typical appliances, such as HVAC systems and and EWHs, as generalized energy storage.

Control information is transferred between OpenDERMS within the control layer and DER devices within the device layer, whether they be simulated or real-world, through the CTA-2045 protocol. DER devices communicate power and voltage data with the circuit layer, which contains a circuit controller that operates a power distribution system simulator. For this study, OpenDSS is employed as the power distribution simulator, but Cyme is also an available option within the testbed. During co-simulation, power and voltage data is captured by a logger and relayed to the visualization and analytics layer, which provides the user with actionable information to analyze the full system.

Communication between the device, circuit, and visualization and analytics layers is achieved through MQTT. MQTT is a lightweight, publish-subscribe network protocol that enables the co-simulation of multiple DERs in a power distribution system simulator [21]. The master controller of the testbed is responsible for co-simulation flow and ensuring that all DER devices, the power distribution system simulator, and the logger are checked in to the MQTT server. Topics, identifiers for data points, are assigned to subscribers and publishers as employed by the MQTT protocol. Each DER within the device layer publishes power data to its assigned topic, and the circuit controller subscribes to the corresponding topics to obtain and apply the power data within OpenDSS. Upon simulation of each timestep, voltage data is published to the appropriately assigned topics and obtained by the correspondingly subscribed DER devices.

Utilizing this DER integration testbed enables distribution-level simulation of DR control schemes and co-simulation of the distribution system simulator, model-in-the-loop (MIL), and other device-level simulators such as EnergyPlus, a whole building energy simulation program. The EPRI's DER integration testbed for energy storage systems is of particular interest for this study as it was utilized for the simulation of an EWH that is treated as an energy storage system [3]. The simulator is capable of various smart functions, such as connection/disconnection, charging/discharging, volt-VAR curve input, and generation level and power factor adjusting. The EWH MIL was simulated in the paper and connected to EPRI's DER integration testbed (Fig. 2).

The Generalized Energy Storage (GES) in a residence includes BESS, EWH, and the HVAC system following the exact definitions from Energy Star specifications [10]. For a BESS, the "current available energy storage capacity", $E_{C,B}$

is for the estimation of available energy storage for potential surplus PV generation and calculated as follows:

$$E_{C,B}(t) = \overline{E_{B,R}} \cdot (SOC_{B,max} - SOC_B(t)), \quad (1)$$

where $\overline{E_{B,R}}$ is the rated energy capacity of the BESS; $SOC_{B,max}$, the maximum allowed state-of-charge (SOC).

Most CA-2045 available EWHs only provide the "energy take" instead of the water temperature inside the tank, which is hard to measure as it is stratified. In this paper, the "energy content of the stored water" for the EWH is defined as:

$$E_W(t) = V\rho c_p \theta_T(t), \quad (2)$$

where V (m^3) is water tank volume; ρ (993 $^{kg}/_{m^3}$), density of water; c_p (4,179 $^{J}/_{kg°C}$), specific heat capacity of water; θ_T (°C), the average temperature in the water tank. Based on (2), the "current available energy storage capacity, $E_{C,W}$" for a water heater is calculated by referring to the set point, as follows:

$$E_{C,W}(t) = \overline{E_{W,S}} - E_W(t), \quad (3)$$

where $\overline{E_{W,S}} = V\rho c_p \theta_{T,S}$ is the maximum energy capacity for the EWH, defined by $\theta_{T,S}$, the set point. The "energy take" is defined as follows:

$$E_{T,W}(t_2 - t_1) = E_W(t_2) - E_W(t_1). \quad (4)$$

The calculation for energy related water heater in (2)–(4) is measured in joule as defined, and which is interchangeable with kWh. The HVAC system is regarded as an energy storage and its equivalent SOC is defined as:

$$SOC_H(t) = \frac{\theta_{max} - \theta_I(t)}{\theta_{max} - \theta_{min}}, \quad (5)$$

where the θ_{max} and θ_{min} are the maximum and minimum room temperature, respectively; θ_I, the indoor temperature, all measured in °C. The energy storage capacity of the HVAC system, $\overline{E_{H,C}}$, is defined as the input electricity needed to change the room temperature from the maximum to the minimum with a fixed outside temperature [8]. The "current available energy storage capacity" for the HVAC system calculated as:

$$E_{C,H}(t) = \overline{E_{H,C}} \cdot (1 - SOC_H(t)). \quad (6)$$

III. Case Study for EWH as Energy Storage

Two cases, which were based on experimental results, were studied to validate the EWH as a MIL in the EPRI's DER integration testbed. In the first case, the simulation results of a resistive EWH was validated against the results from the public report from an EPRI performance test on a CTA-2045 compatible EWH [12]. The "energy take" values for all the DR events were based on the case study published in [12].

The tank temperature and the "energy take" values were calculated as the EWH responded to the "Shed event" signal (Fig. 3). In principle, the "shed" signal postpones the heating process, while the "load up" signal antedates. Detailed

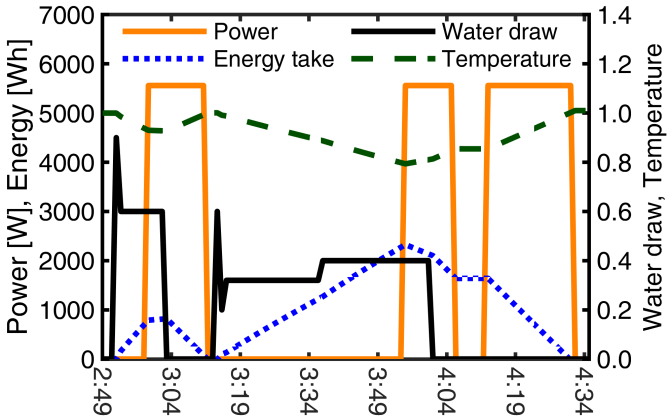

Figure 3. Example of simulated EWH "Shed Event" corresponding to the experimental data illustrated in Fig. 4. Based on DR control signals, the "energy take" capacity was increased from 900Wh to 2,200Wh, resulting in a shift/delay of the water heating process. Both the temperature and water draw are referred in p.u. on the right y-axis, where the base values are 140 F and 1 gallon per minute (GPM), respectively.

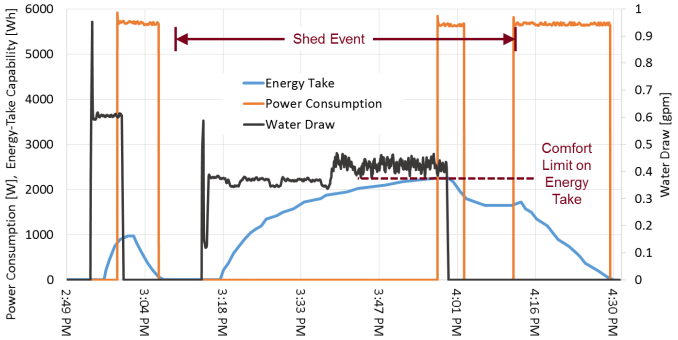

Figure 4. Experimental results reported by NREL/EPRI [12], and employed for the satisfactory validation of the proposed EWH MIL. The "Shed Event" occurs from 3:10 to around 4:10, which causes the "energy take" range to increase and the heating process to be postponed while maintaining occupant comfort.

explanation with mathematical equations and corresponding quantified parameters are presented in the following sections. The temperature and water draw are referred in p.u., where the base values for temperature and hot water flow are 140 F and 1 gallon per minute (GPM), respectively.

The report [12] provides only the visualized results from field measurement, as shown in Fig. 4. The only input for the proposed EWH model was hot water draw, which was estimated visually from Fig. 4. Comparison between Figs. 3 and 4 show satisfactory accuracy of the simulated EWH model with CTA-2045 availability.

The second case was based on the experiment from the EPRI SHINES demonstration, which was launched in 2016 by the DOE to develop and demonstrate technologies that enable sustainable and holistic integration of energy storage with solar PV [22]. In this paper, the EWH loads of the two houses, as well as the BESS, solar PV, pool pump and HVAC were tested in the field. The different EWH loads and BESS charging schedule as well as the corresponding energy and aggregated

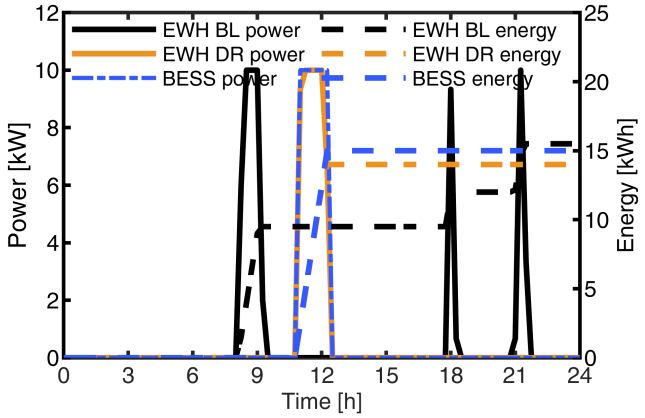

Figure 5. Comparative study of energy storage with BESS and EWH, including typical/normal base line (BL) and DR schedules. For BL operation, the EWH has a morning and two evening peak power cycles. The BESS schedule was adjusted to allow comparison with a EWH study for DR load shifting around noon, which may align well with PV generation, if available.

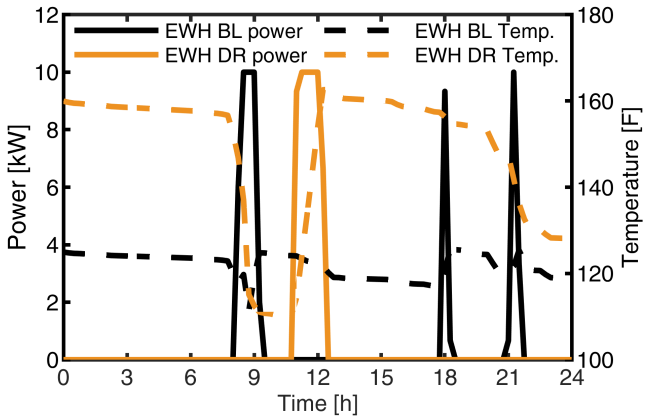

Figure 6. Power draw and water tank temperature for an EWH operating under BL and DR studied schedules. The high water temperature in the tank may be enabled by special mixing valve technologies.

power of the two EWHs are provided for a comparative study (Fig. 5).

The example charging schedule for the BESS resulted in a similar power rating when compared to the EWH DR power (Fig. 6). Mixing valve technology was used to guarantee occupant safety when the temperature in the water tank was high. The EWH under DR can be programmed at night to boost the tank temperature to the same value as the beginning of the day.

The EPRI SHINES demonstration provides timely data with a resolution of 15 minutes for the power flow at the transformer where four houses were connected. Two of the four houses have their own solar PV installations, HVACs, pool pumps, and other non-DER loads monitored by the SHINES project. The non-DER loads of the monitored houses were added to the total power of the other two houses, and were labeled as "uncontrollable loads" at the distribution level (Fig. 7).

The EWH provided the energy storage capacity for the surplus PV generation as the BESS (Fig. 5). The net flow

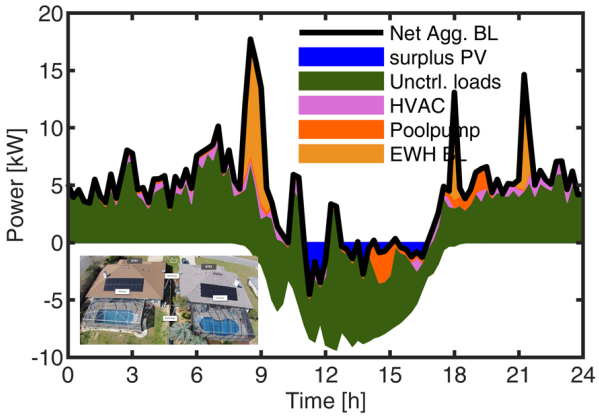

Figure 7. Combined experimental and simulated power flow on an example February day for two smart homes, which are located in Florida and were developed as part of the EPRI SHINES DOE project (photo inset). The EWH simulations were performed with the proposed MIL.

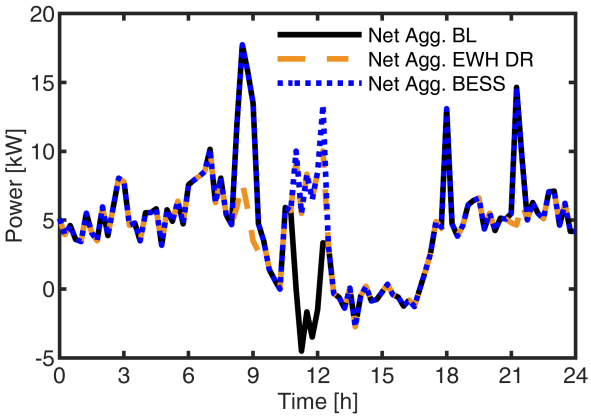

Figure 8. Case studies for the aggregated net power flow at the distribution level. For the proposed control, during the day, a substantial portion of the solar PV generated energy was locally stored in the EWH or BESS.

at the aggregated level was reduced due to the DR control, as shown in Fig. 8. Shifting the EWH load also reduced the peaks in the afternoon and evening.

IV. The Realistic Hot Water Draw and EWH Model with CTA-2045 Control

Hot water draw from the CBECC-Res data set was named as "XDY". X is the number of bedrooms and X∈{1,2,3,4,5}. CBECC-Res water heater draw has three types of days: weekdays (D), weekends (E), and holidays (H). Only type "D" was considered in this study. Y is the Y^{th} profiles for one category and Y∈{0,1,2,3,4,5,6,7,8,9}. The value for Y is only the natural sequence for different profiles and does not attribute to any specific day. For example, "3D8" is the 9^{th} weekday profile for a 3 bedroom house, and it represents a user behavior which could occur at any weekday.

In this study, there were 36 residences with 1 bedroom (Table I), based on the survey published by the United States Census Bureau [23]. Therefore, 36 hot water draw were

Table I
PERCENTAGE AND NUMBER OF HOUSES WITH DIFFERENT BEDROOM NUMBERS

Bedrooms	Percentage (%)	Number
0 & 1	2.1 + 8.2	36
2	25.8	91
3	42.8	151
4	16.7	59
5+	4.5	16

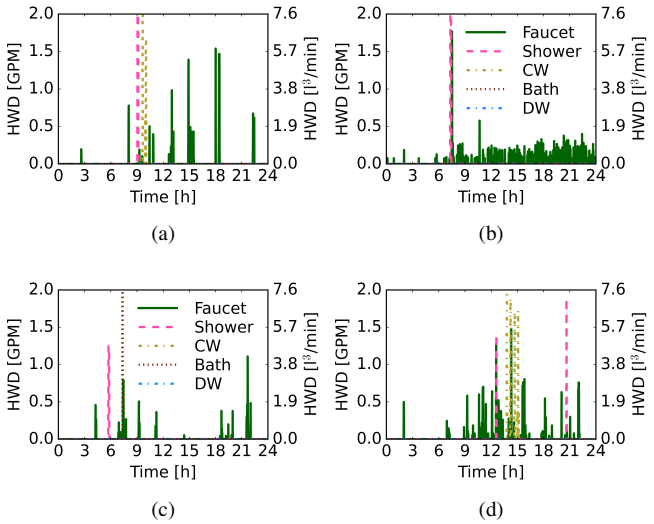

Figure 9. Example hot water draws from CBECC-Res data. Shown are four examples for (a) 1D7; (b) 2D6; (c) 3D3; (d) 4D3.

selected randomly as "1DY" (Y∈{0,1,2,3,4,5,6,7,8,9}) with repetition, i.e., some profiles were selected more than once. Similar procedures were performed for the other residences with more than 1 bedroom, and a total of 353 hot water draw profiles were selected based on the 50 representative hot water profiles from CBECC-Res.

The daily hot water draw profiles in CBECC-Res include the hot water draw (HWD) at different fixtures: faucet, shower, cloth washer (CW), bath, and dishwasher (DW) (Fig. 9). The temperature for hot water and cold water, and the hot water fraction of end use were concluded in [24]. The end use temperature for the fixtures were calculated (Table II).

The hot water flow at the outlet of the water tank was calculated using the water flow balance and energy balance,

Table II
HOT WATER FRACTION AND END USE TEMPERATURE OF FIXTURES.

End use	Hot water fraction	End use Temp. [F]
Faucet	0.50	95
Shower	0.66	105
Clothwasher	0.22	78
Bath	0.66	105
Dishwasher	1.00	125

Table III
WATER HEATER CONDITION AS CHARACTERIZED BY ENERGY TAKE LEVELS

Event	Energy take levels (Q_T) [Wh]	
	Minimum	Maximum
Normal operation	0	300: ≥ 1 GPM 600: ≥ 0.3 GPM 900
Shed	1,800	2,250
Load up	0	300

as follows:

$$\dot{V}_H + \dot{V}_C = \sum \dot{V}_i, \tag{7}$$

$$\dot{V}_H \theta_T(t) + \dot{V}_C \theta_{W,C} = \sum \dot{V}_i \theta_i, \tag{8}$$

where $\dot{V}_H$ is the water flow at the outlet of water tank; $\dot{V}_C$, water flow of cold water; $\dot{V}_i$, water flow at fixture; $\theta_T(t)$, the water temperature in the tank; $\theta_{W,C}$, cold water temperature; θ_i, end use temperature listed in Table II.

The 1R1C gray-box model of EWH is used for the calculation of water temperature with three major effects, i.e., the input electric power, the standby heat loss, and the hot water draw activities, as:

$$C\frac{\mathrm{d}\theta_T(t)}{\mathrm{d}t} = S(t)P_H(t) - \frac{1}{R}[\theta_T(t) - \theta_A] - \rho c_p W(t)\,[\theta_T(t) - \theta_{W,C}], \tag{9}$$

where C and $S(t)$ are the equivalent thermal capacitance and On/Off status, defined respectively, as:

$$C = V \cdot \rho \cdot c_p. \tag{10}$$

$$S(t) = \begin{cases} 0, & \text{if } S(t-1) = 1 \;\&\; E_{T,W}(t) \le Q_{T,min}(t) \\ 1, & \text{if } S(t-1) = 0 \;\&\; E_{T,W}(t) \ge Q_{T,max}(t) \\ S(t-1), & \text{otherwise,} \end{cases} \tag{11}$$

where $Q_{T,min}$ and $Q_{T,max}$ are the energy take levels, which are defined by different DR signals (Table III) [12]. Other parameters are the same as the Table 3 from [25]. The energy take at a given time point $E_{T,W}(t)$ was referred to the starting point of the simulation and (4) is rewritten as:

$$E_{T,W}(t) = E_W(t) - E_W(0). \tag{12}$$

For the Normal operation event, increased hot water flow causes the energy take level to be lower. For the shed event, the energy take levels are much higher to allow for more hot water draw while keep the EWHs Off. The EWH would be On during the shed event when the energy take is too high to

Table IV
EVENT TYPE AND DURATION

Event	Duration
Shed	[7:00,10:00) ∪ [17:00,19:00)
Load up	[6:00,7:00) ∪ [11:00,16:00)
Normal operation	Other time

guarantee the user comfort. For the load up event, the EWH would be On even if the energy take is low.

V. CASE STUDY FOR AGGREGATED EWH POWER

A total of 353 houses were connected to the IEEE 123-bus feeder and the numbers for different house type is presented in Table I, as explained in the previous section. The DR control listed in Table IV was applied to all the EWHs in the same distribution system. The DR control signals were sent to the EWHs via MQTT, as elaborated in previous section. Each EWH has a rated power of 5kW in this study. When most of the EWHs were turned on together, they caused a large peak in aggregated power and increased voltage variation of the distribution power system. This represents the worst scenario for the simulated subdivision, and can be alleviated by a method of sequential control [8]. In this study, all the 353 EHWs were considered as one batch for the sequential control, and therefore, were not subdivided. It should be noted that, regardless of control method, power system voltage remained within the typical 5% tolerance. Effects on voltage are further elaborated in the remainder of this paper.

For utilities serving large areas, the simulated distribution system is one subdivision of the larger system, and the simulated EWHs in this subdivision could be controlled as one batch. Therefore, the peak power for EWHs do not happen at the same time for the upper system. Within the subdivision, a sequential control method spreading out the turning On operation of EWHs, might be used to reduce the peak caused by rebound effect [8].

The initial water temperature in the tanks for all simulated EWHs were evenly distributed between 115F and 135F, noted as $\mathcal{U}(115F, 135F)$. The initial energy take for all simulated EWHs were evenly distributed between 0 and 1000Wh, noted as $\mathcal{U}(0, 1000Wh)$. The simulation results of On/Off status for all 353 EWHs demonstrate the antedated and postponed peak under CTA-2045 control (Fig. 10). The shadowing parts for the controlled case (bottom) indicate the duration when the DR control signals were implemented.

The peaks caused by load up event and the rebound effect are presented in the aggregated power for all the simulated EWHs (Fig. 11). The rebound effect at 9:00 during the shed event was caused by temperature recovering to maintain user comfort. It is observed by comparing the two shed events that the longer the event, the larger the rebound peak afterwards.

For the case without DR (Fig. 12, top), most of the EWHs had the energy take value between [0,1000Wh]. The outliers, which are represented by red dots, were caused by high hot water draw. Most of the outliers appeared in the morning and

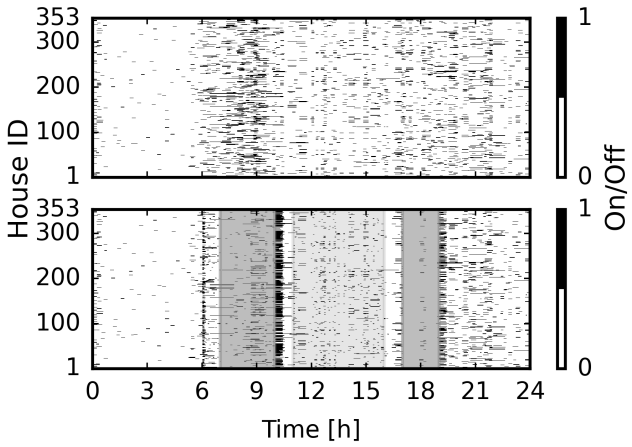

Figure 10. Working status of the EWH without control (top) and with CTA-2045 control (bottom). The shed command in the morning and evening postpone most of the EWHs to be On.

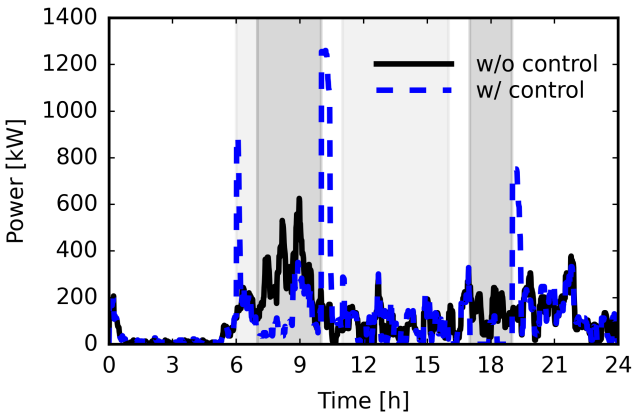

Figure 11. Aggregated power for all the simulated EWHs. The shed command postponed the heating power and reduced the peak power during the DR control period in the morning and evening, but also caused the rebound afterwards.

reflected the high water usage for residences at that time. The minimum energy take values for shed events stayed at 0 instead of 1,800Wh as stated in Table III because some EWHs did not have hot water draw. Therefore, even when the minimum energy take level was high, some EWHs experienced an energy take of approximately 0 until there was hot water usage. This can be observed from 8:00 to 9:00 as the boxes were shifting above.

At 9:30 (Fig. 12, bottom), the upper whisker was lower than that of 9:00 as the EWHs with most energy take were On to maintain user comfort. The 25% percentile and median at 9:30 were higher than those of 9:00, indicating that more EWHs had higher energy take. At 10:00, most EWHs had high energy take and the box moved upward, making the 0 energy take value an outlier. If the shed event had lasted longer, the box would keep moving upward and have the minimum and maximum energy take values as stated in Table III. The shed

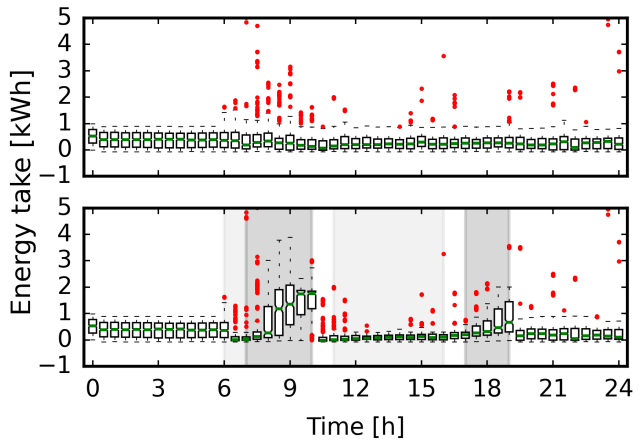

Figure 12. Energy take of the EWHs without control (top) and with CTA-2045 control (bottom). The shed command allowed more energy take while the load up did less.

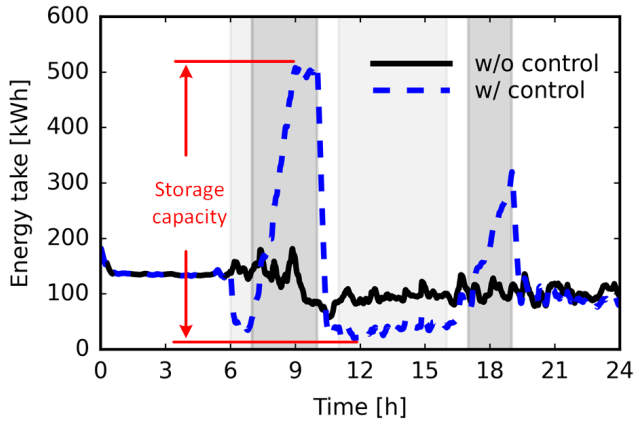

Figure 13. Aggregated energy take for all the simulated EWHs. The shed command in the morning and evening resulted in high energy take. When the load up command was implemented in the afternoon, energy take was kept at a low level. The maximum difference between energy take values indicates the energy storage capacity provided by EWHs.

event in the evening lasted for 2 hours and the forms of boxes behaved similarly to the first 2 hours of the morning shed event (7:00-9:00).

The aggregated energy take rose from approximately 20kWh to 510kWh from 7:00 to 9:00 and then remained at around 500kWh until the shed event ended at 10:00 (Fig. 13). Theoretically, each EWH could have 0 energy take when the shed event starts and have 2,250Wh energy take when the shed event ends. Each EWH could provide a storage capacity of 2,250Wh in theory. Practically, the simulated 353 EWHs were not able to have the aggregated energy take as 794kWh because, at any given time step, there were always some EWHs that did not reach the energy take of 2,250Wh and others that had more than 2,250kWh which were turned On. In this study, all the simulated 353 EWHs provided 490kWh energy storage capacity (Fig. 13), i.e., 1,388Wh per EWH.

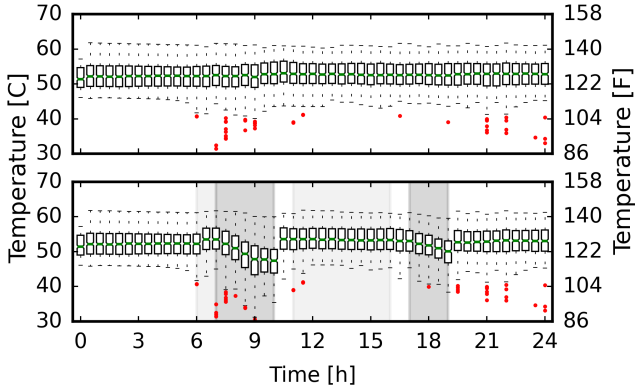

Figure 14. Water temperature in the tank for the EWHs without control (top) and with CTA-2045 control (bottom). The temperature was reduced during the shed event and was maintained high during the load up event in the afternoon.

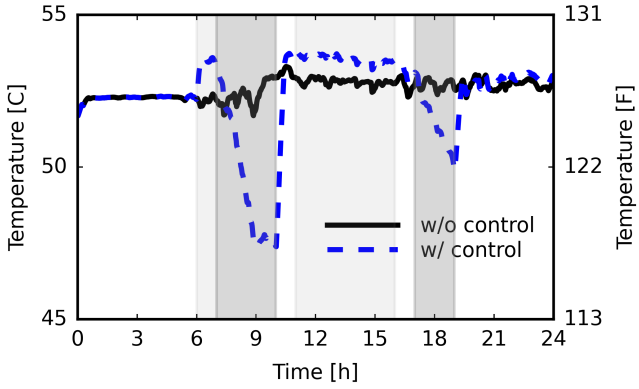

Figure 15. Average tank temperature for all simulated EWHs.

For the case without DR control, the outliers with low temperature appeared from 7:00 to 9:00 due to high hot water flow (Fig. 14, top). The water temperature increased significantly during the first load up event at 6:00. Them temperature at 11:00 did not increase significantly when the load up event started, due to the recovering after the previous shed event. The water temperatures for all EWHs were increased by the load up event in the afternoon, which can be observed clearly from the results at the aggregated level (Fig. 15).

The proposed control scenario reduced the morning and evening peaks, and increased the available energy storage capacity provided by EWHs in the afternoon. In this study, user comfort was considered violated when the energy take value was more than 2,300Wh. For the case without DR response, 96 EWH had the violation for at least 1 minute, and with DR, the number was 171 (Fig. 16).

Further insight revealed that most EWHs had short periods of violation for the without control case, e.g., 72 EWHs violated for less than 15 minutes. With the DR control, 51 EWHs had violation minutes of less than 5. The DR control reduced the violation time for some EWHs because of the preheating process under the load up event starting from

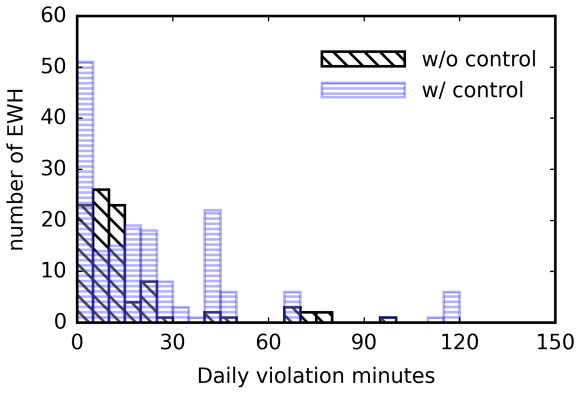

Figure 16. Summary of daily violation minutes for each EWH under the proposed scenario for maximum storage capacity in the afternoon. Three EWHs had daily violation minutes with [40,50) without control, and this number was 18 with control. With DR control, the number of EWHs with more daily violation minutes increased.

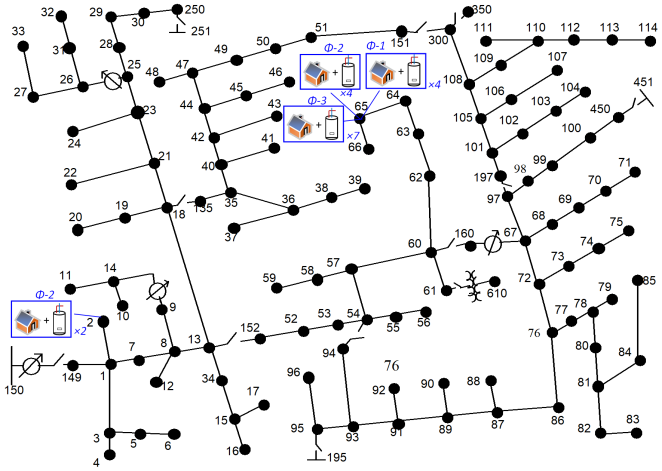

Figure 17. The modified IEEE 123-bus feeder. The original spot loads were replaced by the residential loads, which are comprising of measured data from the SET project and the simulated EWH power.

6:00. The DR control also caused more EWHs to have more violation minutes due to the shed event.

The total violation minutes for all the EWHs was calculated by adding up the violation minutes for each EWH. In total, the case without control had 1,500 violation minutes, and the case with control had 4,033. Given a total number of 353, each EWH experienced around 7 minutes more of comfort violation. This could be solved by increasing the water tank volume and EWH heating rates, or opting out the DR control temporarily when high hot water draw is anticipated.

VI. Case Study for the Power System

The modified IEEE 123-bus feeder [17] was used to simulate the distribution power system for the residential community (Fig. 17). The original spot loads of each node were replaced by the residential loads, which was comprising of the measured data from the Smart Energy Technologies (SET)

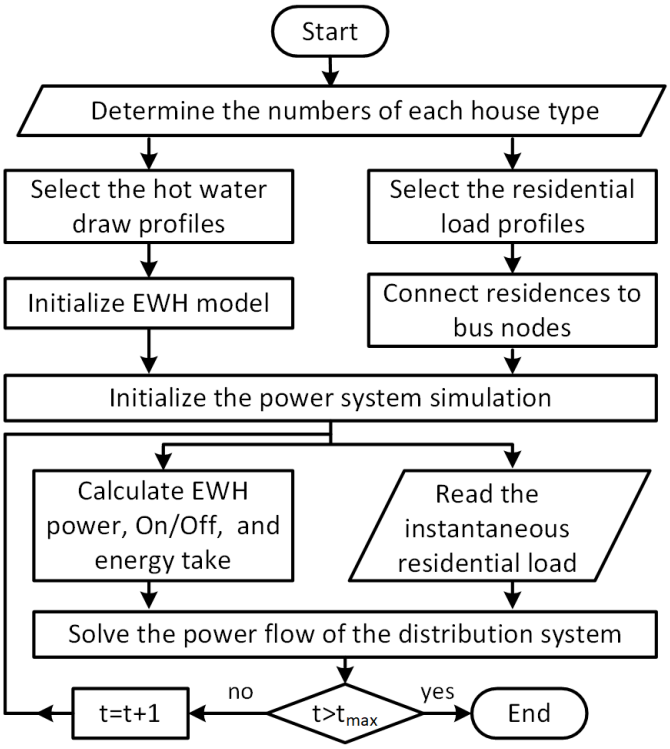

Figure 18. Work flow for the simulation of the distribution power system with realistic residential load and water heater power.

project [19] and simulated EWH power, as illustrated in Fig. 18. This SET project is one of the largest field demonstrators for smart grid in rural US with recorded residential data for more than 5,000 houses, including thermal cycle loads. The additional heat to the room temperature due to water heating was not considered in this study as EWHs had high insulation. It is worth noting that when heat pump water heaters are used, they take energy from the air, resulting in lower room temperature.

Each residence was assumed to have a 10kW maximum, and the default kW value of each node was referred by [17] as "spot loads". Node 2 has 20kW in its phase-2, therefore, 2 houses were connected to Node 2 in phase-2. Similarly to node 65, 4 houses to phase-1, 4 houses to phase-2, and 7 houses to phase-3 were connected.

The house number was rounded to ceiling if the results for dividing the original spot load was not an integer. For example, Phase-1 of node 65 has a spot load of 35kWh. Therefore, 4 houses were connected to phase-1 of node 65. A total of 353 different houses were connected to the modified IEEE 123-bus feeder and their residential profiles were selected from the SET project. In this study, the power factor of 0.95 was assumed for all buses [26].

In this study, the OpenDSS simulator operated in "snap" mode and solved the power flow at each time step with new inputs. The simulation has a resolution of 1-minute and at each time step, power of each EWH was calculated based on the proposed model. The total residential load was comprising of

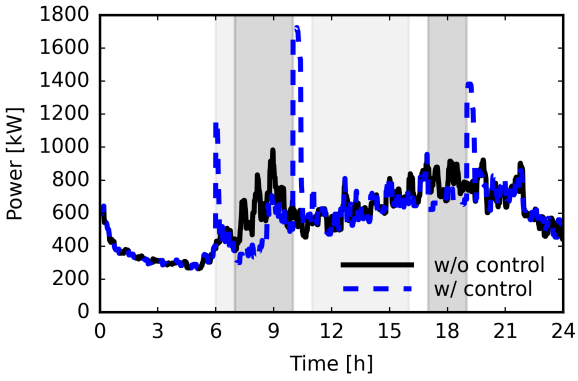

Figure 19. The aggregated residential load for all houses. The shed command postponed the peak power in the morning and evening for this distribution system.

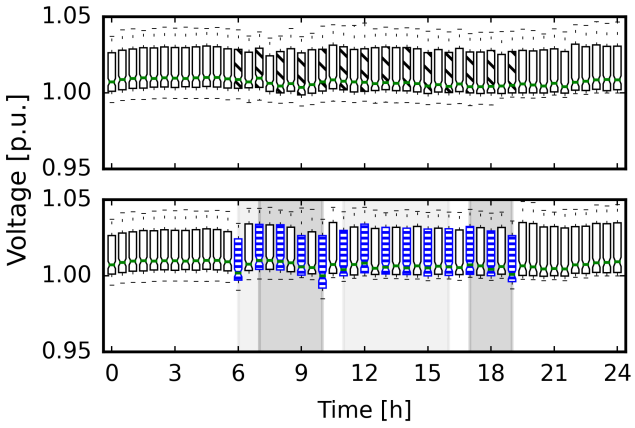

Figure 20. The bus voltages of the IEEE 123-bus system. The boxes during the DR period are marked and compared side-to-side.

the data from SET project and the calculated EWH power. The OpenDSS used the residential loads as inputs and calculated the power and voltage for each bus at each time step.

Outputs from OpenDSS included the total net power flow and voltage at each bus. The total net power flow was used to evaluate the capabilities of residential EWHs for specifically timed peak reduction and for providing energy storage. The voltage of power distribution system was used for monitoring the stability and robustness. It is worth noting that the control of voltage, current, and reactive power is not within the scope of this work.

The total power demand for the simulated IEEE 123-bus (Fig. 19) were calculated by OpenDSS and only the active power (kW) is presented. Peaks were observed at 6:00 when the load up event occurred and at 10:00 and 19:00 when the shed event ended, as has been explained in the previous section (Fig. 11). The peak power from 7:00–10:00 was reduced from 983kW to 706kW, a reduction of 28%.

The simulation results of OpenDSS include 278 voltage values. If a bus has three phases, the voltages of Φ-1, Φ-2, and Φ-3 were recorded separately. All the voltage (Fig. 20) were within the tolerance of 1±0.05 p.u., although large variations were observed at 6:00, 10:00, and 19:00.

For most of the cases, many of the bus voltages were higher than 1 p.u., as the simulated total residential loads were smaller than the spot loads in the original IEEE 123-bus cases. For example, node 2 had an original spot load of 20kW but was replaced by 2 residences, which could not reach such high power demand. Therefore, the voltage for the entire simulated power system was more than 1 p.u. for most of the time.

Bus voltages for selected hours were presented in Fig. 21 to show the impact of DR controls. The samples with the same marks for both cases were taken from Fig. 20. When the load up event started at 6:00, the voltage for most buses dropped as power demand at most buses went high.

The shed event occurred at 7:00, and the bus voltage went higher as power demand reduced. At 9:00, the 75% percentile values were lower, indicating the rebound for some EWHs,

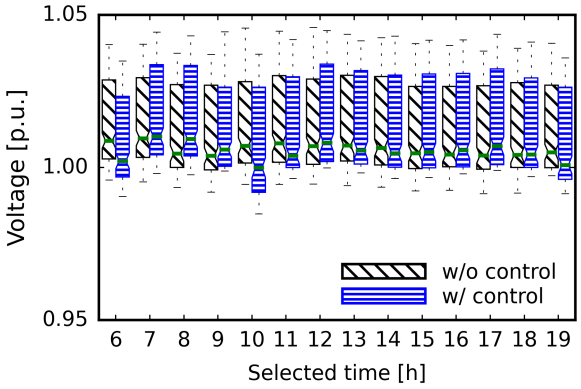

Figure 21. The side-to-side comparison of bus voltages with and without DR control. All the bus voltages were kept within 5% tolerance during the DR events, demonstrating the feasibility of the proposed control.

which were also observed in Figs. 10 and 11. The rebound effect was strong at 10:00 when the shed event ended and large power demand from EWHs brought the voltage down.

During the load up event starting at 11:00, most of the buses had lower voltages. The lower whisker was higher than the without control case due to the rebound effect at 10:00, which prevented some EWHs to be turned On at 11:00. The rebound effect at 10:00 and load up event at 11:00 antedated the water heating process of most EWHs. Therefore, at 12:00, less EWHs were On and the voltages on buses went higher with DR control. A similar cycle was observed at 13:00, 14:00 (antedated operation) and 15:00 (less EWHs were On) during the load up event.

The voltages increased in general during the shed event in the evening from 17:00. Also observed is the rebound effect at 19:00 when the shed event ended. The DR controls shown above caused the violation of the voltages for all buses within the ±0.05p.u. tolerance, even the power demand was almost doubled in this worst scenario (Fig. 19) .

VII. Conclusion

This paper proposes a generalized approach for energy storage that enables all such systems and devices, not only batteries but also electric water heaters (EWHs) and heating, ventilation, and air conditioning (HVAC) systems, to be controlled with the same variables, namely, "energy capacity" and "energy take". Such controls, which were implemented through the Electric Power Research Institute (EPRI) Distributed Energy Resources (DER) integration testbed, comply with the specifications of Energy Star and CTA-2045, which can ensure a platform for industrial and utility adoption. It was found that the example BESS and EWH are comparable when considering their energy content as generalized energy storage (GES) with occupant safety from high water temperatures guaranteed through a mixing valve solution.

A distribution system with 353 residences was simulated using the modified IEEE 123-bus feeder with experimental data and realistic hot water flow. The DR signals complying to CTA-2045 specifications was implemented to all the EWHs for the objectives of reducing the peaks in the morning and evening, and reserving energy storage capacity in the afternoon. The proposed DR control reduced the peak power during the shed event by 28% and enabled an average energy storage of 1,388Wh by each EWH. It should also be noted that due to the shed operation, residences had experienced 7 minutes more than usual during which occupant comfort requirements were not maintained. All the bus voltages were kept within 1±0.05 tolerance throughout the power system even when EWHs were turned On together and the rebounding power increased drastically in the extreme scenario.

VIII. Acknowledgment

The support of the Department of Energy sponsored project DE-EE0009021 led by the Electric Power Research Institute (EPRI) is gratefully acknowledged. The support received by Mr. Evan S. Jones through a Department of Education GAANN Fellowship is also gratefully acknowledged.

References

[1] H. Jain, B. A. Bhatti, T. Wu, B. Mather, and R. Broadwater, "Integrated transmission-and-distribution system modeling of power systems: State-of-the-art and future research diretions," *Energies*, vol. 14, no. 1, p. 12, 2021.

[2] J. Anandan, "EPRI's DER integration testbed and toolkit," Electric Power Research Institute (EPRI), Tech. Rep. 3002016138, 2019.

[3] B. Ealey, "Overview of epri's der simulation tool for emulating smart solar inverters and energy storage systems on communication networks," Electric Power Research Institute (EPRI), Tech. Rep. 3002013622, 2018.

[4] A. Pratt, M. Ruth, D. Krishnamurthy, B. Sparn, M. Lunacek, W. Jones, S. Mittal, H. Wu, and J. Marks, "Hardware-in-the-loop simulation of a distribution system with air conditioners under model predictive control," in *2017 IEEE Power & Energy Society General Meeting*. IEEE, 2017, pp. 1–5.

[5] J. Lian, Y. Tang, J. Fuller, K. Kalsi, and N. Wang, "Behind-the-meter transactive control approach for home energy management system," in *2018 IEEE Power Energy Society General Meeting (PESGM)*, 2018, pp. 1–5.

[6] A. Al-Fuqaha, M. Guizani, M. Mohammadi, M. Aledhari, and M. Ayyash, "Internet of things: A survey on enabling technologies, protocols, and applications," *IEEE communications surveys & tutorials*, vol. 17, no. 4, pp. 2347–2376, 2015.

[7] X. Li, L. Nie, S. Chen, D. Zhan, and X. Xu, "An iot service framework for smart home: Case study on hem," in *2015 IEEE International Conference on Mobile Services*. IEEE, 2015, pp. 438–445.

[8] H. Gong, E. S. Jones, R. E. Alden, A. G. Frye, D. Colliver, and D. M. Ionel, "Virtual power plant control for large residential communities using hvac systems for energy storage," *IEEE Transactions on Industry Applications*, vol. 58, no. 1, pp. 622–633, 2022.

[9] H. Gong, V. Rallabandi, D. M. Ionel, D. Colliver, S. Duerr, and C. Ababei, "Dynamic modeling and optimal design for net zero energy houses including hybrid electric and thermal energy storage," *IEEE Transactions on Industry Applications*, vol. 56, no. 4, pp. 4102–4113, 2020.

[10] "Energy star water heaters - test method to validate demand response," https://www.energystar.gov/products/spec/residential_water_heaters_specification_version_3_0_pd, accessed: 2022-7-25.

[11] "CTA standard: Modular communications interface for energy management," Consumer Technology Association (CTA), Tech. Rep., 2020.

[12] C.Thomas, "Performance test results: CTA-2045 water heater," Electric Power Research Institute (EPRI), Tech. Rep. 3002011760, 2017.

[13] "CTA-2045 water heater demonstration report including a business case for CTA-2045 market transformation," Bonneville Power Administration (BPA), Tech. Rep. BPA Technology Innovation Project 336, 2018.

[14] F. Sossan, A. M. Kosek, S. Martinenas, M. Marinelli, and H. Bindner, "Scheduling of domestic water heater power demand for maximizing pv self-consumption using model predictive control," in *IEEE PES ISGT Europe 2013*, 2013, pp. 1–5.

[15] "CBECC-Res Compliance Software Project," http://www.bwilcox.com/BEES/cbecc2019.html, accessed: 2020-08-04.

[16] K. P. Schneider, B. A. Mather, B. C. Pal, C.-W. Ten, G. J. Shirek, H. Zhu, J. C. Fuller, J. L. R. Pereira, L. F. Ochoa, L. R. de Araujo, R. C. Dugan, S. Matthias, S. Paudyal, T. E. McDermott, and W. Kersting, "Analytic considerations and design basis for the ieee distribution test feeders," *IEEE Transactions on Power Systems*, vol. 33, no. 3, pp. 3181–3188, 2018.

[17] "IEEE PES Test Feeder: 123-BUS Feeder," https://cmte.ieee.org/pes-testfeeders/resources/, accessed: 2022-7-25.

[18] K. Marnell, C. Eustis, and R. B. Bass, "Resource study of large-scale electric water heater aggregation," *IEEE Open Access Journal of Power and Energy*, vol. 7, pp. 82–90, 2020.

[19] H. Gong, V. Rallabandi, M. L. McIntyre, E. Hossain, and D. M. Ionel, "Peak reduction and long term load forecasting for large residential communities including smart homes with energy storage," *IEEE Access*, vol. 9, pp. 19 345–19 355, 2021.

[20] H. Gong, E. S. Jones, A. Jakaria, A. Huque, A. Renjit, and D. M. Ionel, "Generalized energy storage model-in-the-loop suitable for energy star and cta-2045 control types," in *2021 IEEE Energy Conversion Congress and Exposition (ECCE)*. IEEE, 2021, pp. 814–818.

[21] N. Tansangwom and W. Pora, "Development of smart water heater complied with mqtt and echonet lite protocols," in *2018 IEEE International Conference on Consumer Electronics - Asia (ICCE-Asia)*, 2018, pp. 206–212.

[22] A. Magerko, A. Huque, T. Hubert, A. Cortes, and R. May, "Enabling behind-the-meter distributed energy resources to provide grid services," in *2019 IEEE 46th Photovoltaic Specialists Conference (PVSC)*. IEEE, 2019, pp. 2064–2071.

[23] "United states census bureau: Numer of housing unites," https://data.census.gov/cedsci/table?q=bedrooms&tid=ACSDT1Y2018.B25041&vintage=2018&hidePreview=true&g=400C100US45640&moe=false&tp=false, accessed: 2022-7-25.

[24] N. Kruis, P. B. Wilcox, J. Lutz, and C. Barnaby, "Development of realistic water draw profiles for california residential water heating energy estimation," in *Proceedings of the 15th IBPSA Conference San Francisco, CA, USA*, 2017.

[25] H. Gong, T. Rooney, O. M. Akeyo, B. T. Branecky, and D. M. Ionel, "Equivalent electric and heat-pump water heater models for aggregated community-level demand response virtual power plant controls," *IEEE Access*, vol. 9, pp. 141 233–141 244, 2021.

[26] M. Pipattanasomporn, M. Kuzlu, S. Rahman, and Y. Teklu, "Load profiles of selected major household appliances and their demand response opportunities," *IEEE Transactions on Smart Grid*, vol. 5, no. 2, pp. 742–750, 2013.

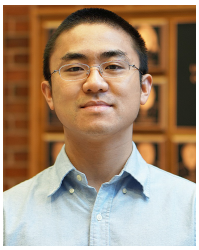

Huangjie Gong (S'18) received the B.Eng. degree in automation from Harbin Engineering University, Harbin, China, in 2013 and the M.S. degree in control theory and control engineering from Southwest Jiaotong University, Chengdu, China, in 2016. Since 2017 he is a Ph.D. student in the SPARK Laboratory, ECE Department at University of Kentucky, Lexington, KY, where he has been working on research projects sponsored by DOE, NSF, Electric Power Research Institute (EPRI), industry and utilities. He is the main developer of a large-scale co-simulation software framework for energy in buildings and power flow in electric distribution systems. In 2021, he was a graduate student intern with the National Renewable Energy Laboratory (NREL). He is an executive committee member for the joint student chapter at UK and a member of PES renewable energy generation subcommittee. His research interests include renewable energy integration, modeling and control of energy storage, batteries, water heaters, HVAC systems, EV, net zero energy (NZE) buildings, and microgrids.

Evan S. Jones received B.S. degrees in electrical engineering and computer engineering with a minor in computer science from the University of Kentucky (UK), Lexington, Kentucky, USA in 2019. He is currently a PhD student in the SPARK Laboratory and a U.S. Department of Education GAANN Ph.D. Fellow. During his undergraduate studies, he was an L. Stanley Pigman Scholar, an IEEE PES Plus Scholarship recipient, and a student engineer for the EKPC utility. At UK, he worked on research projects sponsored by the Department of Energy (DOE), Electric Power Research Institute (EPRI), and the TVA and LG&E and KU utilities. He served as the Vice Chair for the joint student chapter of IEEE PES and IAS at UK. His research interests include building energy models (BEMs), virtual power plants (VPPs), electric power systems, and renewable energy generation and integration.

A H M Jakaria AHM Jakaria works as an Engineer/Scientist III at the Electric Power Research Institute (EPRI) in the Distributed Energy Resources (DER) group. Smart DER communication techniques for DER management systems is one of his primary responsibilities. He performs research and development for software and hardware, focusing on communication management in smart electric grids, as well as efficient technologies for collecting information from remote smart systems. Jakaria received his M.S. and Ph.D. in Computer Science from Tennessee Tech University at Cookeville, TN, in 2019 and 2020, respectively. During his graduate studies, he was actively involved with the Center for Energy Systems Research (CESR), and Cybersecurity Education, Research and Outreach Center (CEROC) at Tennessee Tech as a graduate research assistant.

Aminul Huque Dr. Aminul Huque is currently working as a Program Manager at Electric Power Research Institute (EPRI). He manages smart inverter and grid support technology research at EPRI which supports safe and reliable integration of renewables on the power gird. Dr. Huque leads projects that research, develop, and demonstrate solutions to gird integration challenges associated with higher penetration of distributed energy resources (DERs), including solar Photovoltaic (PV), energy storage, vehicle-to-grid, and controllable loads. He is a key contributor of DER interconnection standards like IEEE 1547. Dr. Huque received a PhD from the University of Tennessee at Knoxville (Tennessee, USA) and an MSc from the Imperial College London (London, UK) in 2010 and 2003 respectively.

Ajit Renjit Dr. Renjit manages and conducts EPRI's strategic research on DER Management Systems developing, implementing and evaluating control systems for the integration of DERs, and microgrids. He has successfully led several NYSERDA and California Energy Commission (CEC) funded projects on grid integration and management of DER. Dr. Renjit also manages EPRI's TSO/DSO Coordination Working Group that aims to address the needs of FERC Order 2222 through a broad stakeholder consensus process which includes, DSOs, ISOs/RTOs, DERMS vendors, academia and national labs. He has hands on experience with evaluating commercial DER, microgrid controllers and DERMS in the lab and field. Before joining EPRI, he worked as a power systems engineer at Spirae in Fort Collins, Colorado. Prior to that, he worked with Siemens, India as a power system engineer. He holds a PhD in Electrical Engineering on Power Systems from the Ohio State University.

Dan M. Ionel (M'91–SM'01–F'13) received the M.Eng. and Ph.D. degrees in electrical engineering from the Polytechnic University of Bucharest, Bucharest, Romania. His doctoral program included a Leverhulme Visiting Fellowship with the University of Bath, Bath, U.K and he later was a Postdoctoral Researcher with the SPEED Laboratory, University of Glasgow, Glasgow, U.K.

Dr. Ionel is a professor of electrical engineering and the L. Stanley Pigman Chair in Power with the University of Kentucky, Lexington, KY, USA, where he is also the Director of the Power and Energy Institute of Kentucky and of the SPARK Laboratory. He previously worked in industry for more than 20 years. Dr. Ionel's current research group projects on smart grid and buildings, and integration of distributed renewable energy resources and energy storage in the electric power systems are sponsored by NSF, DOE, industry and utilities. He published more than 200 technical papers, including some that received IEEE awards, was granted more than 30 patents, and is co-author and co-editor of the book "Renewable Energy Devices and Systems – Simulations with MATLAB and ANSYS", CRC Press.

Dr. Ionel received the IEEE PES Veinott Award, was the Inaugural Chair of the IEEE IAS Renewable and Sustainable Energy Conversion Systems Committee, an Editor for the IEEE TRANSACTIONS ON SUSTAINABLE ENERGY, and the Technical Program Chair for IEEE ECCE 2016. He is the Editor in-Chief for the Electric Power Components and Systems Journal, and the Chair of the Steering Committee for IEEE IEMDC.